

MINISTRY OF EDUCATION  
AND TRAINING

VIETNAM ACADEMY OF  
SCIENCE AND TECHNOLOGY

**GRADUATE UNIVERSITY SCIENCE AND TECHNOLOGY**

-----

**NGUYEN CAO HIEN**

**SYNTHESIS OF NANOPARTICLES BASED ON  
 $\beta$ -CYCLODEXTRIN AND MODIFIED  
 $\beta$ -CYCLODEXTRIN AS CANCER DRUG CARRIERS**

Major: Organic Chemistry

Code: 9.44.01.14

**SUMMARY OF CHEMICAL DOCTORAL THESIS**

HO CHI MINH CITY, 2023

This thesis was completed at: Graduate University Science and Technology - Vietnam Academy of Science and Technology

Supervisors:

1. Assoc. Prof. Dr. Dang Chi Hien

2. Prof. Dr. Sc. Nguyen Cong Hao

Reviewer 1:

Reviewer 2:

Reviewer 3:

This thesis will be evaluated by the evaluation committee of doctoral dissertation, taking place at Institute of Chemical Technology - Vietnam Academy of Science and Technology, on .....2023

This thesis information can be found in:

- The library of the Graduate University of Science and Technology, Vietnam Academy of Science and Technology
- The National Library of Vietnam

## INTRODUCTION

### 1. The urgency of this study

Cyclodextrin derivatives (CD-x) have really attracted the attention of scientists since the early years of the twentieth century because of their outstanding features that significantly improve the limitations of the original CD, demonstrating an important role in advanced application areas. Having come a long way in development, today the number of known cyclodextrin derivatives exceeds 11,000 with multiple reaction pathways that can lead to the desired derivatives. A truly significant milestone in the history of CD's applied research was recognized by the first publication (1990) of a nanomaterial with the scientific name "nanosponge" (due to its nanosponge-like structure) based on the combination of CD and another polymer. The combination of CD and nanotechnology has opened up potential prospects with great advances being made in various fields such as agriculture, pharmaceuticals, biomedical materials and biotechnology. Subsequent studies on cyclodextrin-based nanosponges (CD-NSs) have been successfully tested on many different polymer substrates, the results also show that among the common CDs ( $\alpha$ ,  $\beta$  and  $\gamma$ ) there are  $\beta$ -CD and its derivatives ( $\beta$ -CD-x) are increasingly used because of the advantages of safety, biocompatibility and reasonable cost.

Recently, many studies on hybrid nanogels or nanosystems based on  $\beta$ -CD and their derivatives ( $\beta$ -CD-x) have shown that the complexation efficiency as well as the stability of the resistant complex significantly influenced by the stereochemistry of the  $\beta$ -CD-x molecule and the polarity of the functional groups on the outer surface of the truncated cone. Although many efforts have been made over the years to understand the interaction mechanism in CD-NSs as well as the capture mechanism of "guest" molecules of nanosponges, up to now, no conclusion has been reached. clear . There are many views that: drugs or "guest" molecules are not only enclosed within the "central cavity" of the  $\beta$ -CD-x molecule but also on the hydrophilic outer

surface or distributed throughout the matrix polymer network. . Some of our recent studies on nanogel materials based on  $\beta$ -CD and HPCD have given results consistent with the above statement. Continuing the research series with the desire to develop a new group of materials applied in modern medicine and at the same time provide more scientific data on the role of  $\beta$ -CD and some derivatives in drug delivery efficiency, we propose the topic "*Synthesis of nanoparticles based on  $\beta$ -cyclodextrin and modified  $\beta$ -cyclodextrin as cancer drug carriers*" for this thesis.

## **2. Objectives of the thesis**

Research on synthesis of nanomaterials based on  $\beta$ -CD and modified  $\beta$ -CD. Application of the cancer drug delivery trial 5-Fluorouracil.

## **3. Main research contents**

1. Synthesis of some amine derivatives of  $\beta$ -cyclodextrin
2. Preparation of nanomaterials based on CD and modified CD
3. Investigation of optimal conditions for the synthesis of nanosystems carrying the cancer drug 5-Fluorouracil.
4. Determine the structure, morphology and characteristics of synthesized nanosystems.
5. Studying the effect of CD derivatives on particle size, carrying capacity and release of cancer drug 5-Fluorouracil.
6. Study on cytotoxicity of drug-free nanosystems and evaluate anti-cancer activity of drug-carrying nanosystems.

## **CHAPTER 1: OVERVIEW**

This section presents an overview of  $\beta$ -cyclodextrin and cyclodextrin-based drug delivery materials.

## CHAPTER 2: EXPERIMENTAL

### 2.1. Chemicals and materials

The solvents and chemicals used in the experiments are presented in this section.

### 2.2. Synthesis of amine derivatives of $\beta$ -cyclodextrin

The procedure was initiated with Tosylimidazole preconditioning before  $\beta$ -CD denaturation was performed.

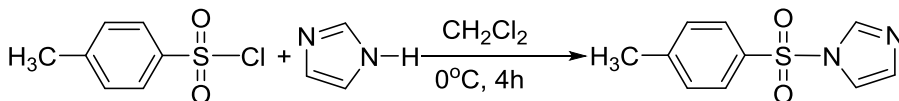


**Figure 2. 1.** Scheme of the *TsIm* synthesis reaction.

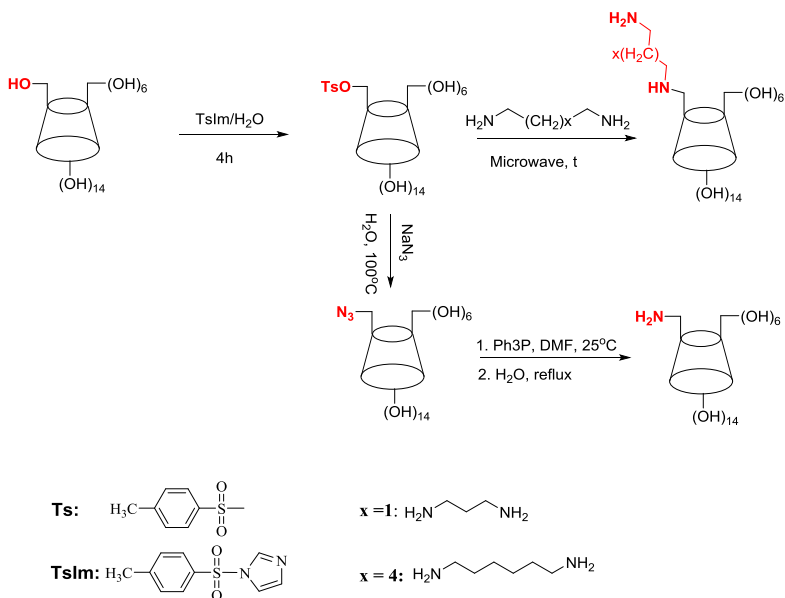


**Figure 2.2.** Schematic diagram of the synthesis of amine derivatives of  $\beta$ -cyclodextrin

Amino derivatives of  $\beta$ -cyclodextrin include: Mono-6-amino-deoxy-6- $\beta$ -cyclodextrin; Mono-(6-(1,3-trimethylenediamine)-6-deoxy)- $\beta$ -cyclodextrin; Mono-(6-(1,6-hexamethylenediamine)-6-deoxy)- $\beta$ -cyclodextrin was synthesized from  $\beta$ -CD. The reactions are described in the diagram 2.2

## 2.3. Preparation of nanomaterials based on modified $\beta$ -CD and $\beta$ -CD

### 2.3.1 $\beta$ -CD-x/alginate nanogel materials:

Slowly add  $\text{CaCl}_2$  solution (10 mg.  $\text{mL}^{-1}$ ) to erlen containing alginate solution (10 mg  $\text{mL}^{-1}$ ), stirring at 1200 rpm for 90 minutes. The stirring solution was sonicated without heating for 60 min before gel stabilization was performed for 24h at room temperature. Next, the solution was centrifuged at 4000 rpm for 15 min, the aliquot from the gel layer was removed, and the gel was washed three times with deionized water. The gel obtained after centrifugation was added to erlen and stirred with a small amount of distilled water, slowly adding  $\beta$ -CD-x solution (2 mg.  $\text{mL}^{-1}$ ) to the erlen in specified volumes (in proportion). survey) and stirred at 1200 rpm for 90 min. After stirring, the solution was sonicated without heating for 60 min. After sonication, the gel stabilization was continued for 24h at room temperature.

The solution was then centrifuged at 4000 rpm for 15 min, the aliquot from the gel was removed, and the gel was rinsed with deionized water. The gel washing process was repeated twice, gel separation and freeze drying for 20 h obtained nanocomposites.

The nanocomposite samples after sublimation drying are weighed to determine the absolute dry weight and calculate the efficiency according to the formula:

$$H_{\text{NPs}}(\%) = \frac{m_k}{m_o} \cdot 100\% \quad (2-2)$$

In there:

$m_k$  is the mass of the sample after lyophilization (mg)

$m_o$  is the total mass of the starting reactants (mg)

### **2.3.2. Hybrid material with gold nanoparticles**

AuNPs/CD-x nanoparticles were synthesized by reducing HAuCl<sub>4</sub> by β-CD-x in alkaline solution under ultrasonic conditions. HAuCl<sub>4</sub> (11.85 mL, 0.16 mM) and β-CD-x (3 mL) at different concentrations were added to a brown reaction flask (50 mL) and stirred at room temperature. To optimize the nanoparticle synthesis, different reaction conditions including β-CD-x concentration, pH, temperature and time were investigated under ultrasonic radiation (200 W, 40 kHz). Skymen Ultrasonic Cleaner 6.5L Jp-031). The pH values of the solution in the range of 8 - 12 were adjusted using a solution of NaOH (1M). The pink color of the solution confirms the formation of AuNPs. The optimization condition was investigated using UV-Vis measurement.

## **2.4 Synthesis of drug-loading nanomaterials**

### ***Synthesis of β-CD-x/alginate nanosystems carrying 5-FU***

The 5-FU@β-CD-x/Alg nanocomposite was formed through an ionotropic gelation mechanism. β-CD-x molecules possess negatively charged groups that can interact to form cross-links between Ca<sup>2+</sup> and alginate ions in gelispheres to form water-dispersible nanocomposites. 5-FU drug can be encapsulated in a polysaccharide matrix through the binding of Ca<sup>2+</sup> ions with functional groups in the alginate molecule or in the central cavity of the β-CD-x molecule..

Nanocomposite 5-FU@β-CD-x/Alg is easily recovered using centrifugation, freeze-drying processes. Because drug content can significantly affect nanocomposite synthesis efficiency, drug loading has been investigated with different ratios between drug weight and carrier mass. Drug loading efficiency (%DL) and drug complexing capacity (%EE) were used to evaluate the synthesis performance. The best morphological nanocomposites are used to investigate the physicochemical and kinetic properties. drug release *in vitro*.

To determine the complexing efficiency of the drug (%EE) and the drug carrying capacity of the material (%DL), we used an indirect method through the loss of 5-FU in the centrifuge water. The amount of 5-FU drug that did not participate in complexing with the material was calculated based on the standard curve equation built with 10 different concentrations of 5-FU and determined by UV-Vis molecular absorption spectroscopy method. at 266 nm.

The complexation efficiency of 5-FU and tolerability on the materials were calculated according to equations 2.3 and 2.4, respectively.

$$EE (\%) = \frac{W_{total\ 5-FU} - W_{free\ 5-FU}}{W_{total\ 5-FU}} \times 100\% \quad (2.3)$$

$$DL (\%) = \frac{W_{total\ 5-FU} - W_{free\ 5-FU}}{W_{nanocomposite}} \times 100\% \quad (2.4)$$

### ***Procedure for loading 5-FU drug onto AuNPs/CD-x nanosystems***

The antineoplastic drug 5-fluorouracil (5-FU) was successfully distributed into AuNPs/CD-x nanocomposites. The aim of this work was to investigate the effect of different functional groups on the drug loading efficiency of AuNPs/CD-x materials. Nanocomposites AuNPs/CD-x are easily fabricated under the help of ultrasound as recently reported by us. A similar procedure was used to prepare all nanocomposites performed at pH 10, 80°C and irradiated continuously for 30 min. Recent studies have shown that  $\beta$ -CD can easily encapsulate 5-FU in the solid state, however, 5-FU complexation when performed in aqueous solution gives low efficiency relative to stability. determination of the complex. Therefore, in this procedure, the empty nanocomposite solution was cleaned and lyophilized prior to drug loading. The pink solid nanocomposite material was obtained with the maximum absorbance at 525 nm in the UV-Vis spectrum. The antineoplastic agent 5-FU was then introduced into the nanocomposite by a simple stirring process for



24h. The mixture was centrifuged and then sublimed to obtain a blue solid that absorbed at a wavelength of about 550 nm.

The nanocomposite product was obtained by lyophilization (-80 °C, 10 h). To determine the complexation efficiency of the drug (EE%) and the drug carrying capacity of the material (DL%), we used an indirect method through the 5-FU content in the centrifuge water. The amount of 5-FU drug lost in the centrifuge water (not participating in complexing with the material) was calculated based on the standard curve equation built with 5 different concentrations of 5-FU and determined by photometric method. UV-Vis molecular absorption spectrum at 266 nm. Complexing efficiency and drug loading capacity were calculated according to equations (2.3) and (2.4).

## **2.5 Structure, morphology and characteristics of nanocomposites**

The presence of functional groups in the composition of nanosystems was analyzed through FT-IR spectroscopy performed on a spectrophotometer (Brucker, Germany) with a wavelength range of 4000 -500  $\text{cm}^{-1}$  and a resolution of 0.5  $\text{cm}^{-1}$ .

The particle size distribution and morphology of the nanocomposites were evaluated by TEM images (S-4800 JEOL JEM1400) set at an accelerating voltage of 120 kV and FESEM (S-4800 HI-9057-0006). Zeta potential is used to determine the charge at phase interfaces and molecular vibrations, while DLS is used to determine the particle size distribution in the colloidal solution. Measurements were performed on nanoPartica Horiba SZ-100 device (Japan) with a solution concentration of 0.5 mg/mL. The Zeta potential was measured with an applied voltage of 3.3 V at 25 °C and the DLS was performed at an angle of 173 °.

The composition, crystal structure characteristics of the drug samples, materials and nanocomposites were determined by X-ray diffraction (XRD) on an X-ray diffractometer (Bruker, Model-D8 Advance).

The thermal properties of the samples of reagents, drugs and nanocomposites were subjected to thermal gravimetric analysis (TGA) and thermal differential scanning (DSC) performed on a LabSys Evo 1600 thermal analyzer (SETARAM, France) at a range of temperatures. 30–800 °C, heating rate 10<sup>0</sup>C/min in air.

## 2.6 Release the drug

Drug release studies were performed in a simulated physiological environment (phosphate-buffered saline at pH 7.4 and 1.2). Drug release efficacy was assessed using a 5 mL dialysate bag (molecular weight range from 3,000 to 5,000 Da). Before testing, the dialysate bags were soaked for 12 h in release medium. A solution mixture of drug-carrying nanocomposites (3 mg) and release medium (3 mL) was added to the dialysis bag with the ends secured. The dialysate bag is dipped in 12 mL of release medium maintained at 37°C and gently stirred. To detect drug release, a small amount (0.5 mL) was taken at different times 1 h, 2 h, 4 h, 8 h, 12 h, 24 h, 48 h and 72 h and then immediately changed solution outside with the same volume of new medium. The recovered samples were analyzed by UV-Vis spectroscopy. The tests were performed in triplicate. The drug release pattern is plotted as the relative release percentage of the drug over time. The same procedure was performed for the nanoblank samples as the reference standard. The drug release result is calculated according to the formula (2.5) from different media.

$$release (\%) = \frac{Amount\ of\ 5-FU\ at\ time\ t}{Amount\ of\ 5-FU\ at\ time\ t=0} \times 100\% \quad (2.5)$$

The kinetics of the drug release processes are compared with theoretical models including: zero order (Equation 2.6), first order (Equation 2.7), Hixson-Crowell (Equation 2.8), Higuchi (Equation 2.9) and Korsmeyer-Peppas (Equation 2.10).

Where  $f_t$  is the amount of 5-FU drug released at a specified time  $t$ ,  $f_0$  is the initial amount of drug in the nanocomposite,  $n$  is the diffusion exponent, and  $k_0$ ,  $k_1$ ,  $k_H$ ,  $k_{HC}$  and  $k_{KP}$  are constants. release numbers corresponding to the equations.

### 2.3.6 Cytotoxicity assay

Fibroblasts and MCF-7 cells (HTB-22) were provided and cultured by the University of Natural Sciences, Vietnam National University, Ho Chi Minh City. Cells were cultured at 37°C and 5% CO in Eagle's minimum essential medium (EMEM) supplemented with 20 mM HEPES (Sigma), 0.025 µg/mL amphotericin B (Sigma), 2 mM L-glutamine (Sigma), and 0.025 µg/mL amphotericin B (Sigma). Sigma), 100 IU/mL penicillin G (Sigma), 100 µg/mL streptomycin (Sigma) and 10% (v/v) FBS (Sigma). Nanosamples including: Hollow material, drug delivery material and solution after drug release were used for cytotoxicity testing.

## CHAPTER 3: RESULTS AND DISCUSSION

### 3.1 Synthesis of β-CD derivatives

#### 3.1.1 Synthesis of mono-6-amino-deoxy-6-β-cyclodextrin (CD-NH<sub>2</sub>)

Efficiency: 93.96%.

Melting point 215-216 °C.

ESI-MS ( $m/z$ ):  $[M+H]^+ = 1214,3676$  tương ứng với  $M = 1214$  (C<sub>42</sub>H<sub>71</sub>O<sub>39</sub>N).

IR ( $cm^{-1}$ ,  $KBr$ ): 3428 (O-H), 3389 (N-H), 2925 (C-H), 1029 (C-O).

<sup>1</sup>H-NMR (500 MHz, DMSO-*d*<sub>6</sub>, ppm): δ 5,75-5,66 (*m*, 14H, 1OH<sub>2</sub>, 1OH<sub>3</sub>, 6OH<sub>2</sub>', 6OH<sub>3</sub>'), 4,83 (*d*, 7H, *J* = 5 Hz, H<sub>1</sub>, 6H<sub>1</sub>'), 4,47 (*s*, 6H, 6OH<sub>6</sub>), 3,69-3,53 (*m*, 28H, H<sub>2</sub>, H<sub>3</sub>, H<sub>4</sub>, H<sub>5</sub>, 6H<sub>2</sub>', 6H<sub>3</sub>', 6H<sub>4</sub>', 6H<sub>5</sub>'), 3,35-3,27 (*m*, 16H, 12H<sub>6</sub>, 2H<sub>6</sub>', NH<sub>2</sub>).

<sup>13</sup>C-NMR (125 MHz, DMSO-*d*<sub>6</sub>, ppm): δ 101,97 (C-1); 81,5 (C-2, C-3); 73,0; 72,3; 72,0 (C-4); 68,7 (C-6'); 59,9 (C-5, C-6).

### 3.1.2 Synthesis of mono-6-(1,3-trimethylenediamine)-6-deoxy- $\beta$ -cyclodextrin

Efficiency: 76,5 %.

Appearance: The product is a white crystalline solid.

Melting point: 259°C-260°C

TLC: butanol:ethanol:water:ammonia (5:4:3:5), color and TLC plates using anisaldehyde reagent showed  $R_f = 0,49$ .

QTOF-MS ( $m/z$ ): 1191,45087 corresponding to  $M = 1190,4436$  (CTPT:  $C_{45}H_{79}N_2O_{34}$ ).

IR ( $cm^{-1}$ , KBr): 3417 (O-H), 1642 và 1525 (N-H), 2927 (C-H), 1031 (C-O).

$^1H$ -NMR (500 MHz,  $D_2O$ , ppm):  $\delta$  5,05 (s, 7H, 6H1', 1H1), 3,94-3,82 (m, 32H, 6(OH)6', 1(OH)2, 6(OH)2', 1(OH)3, 6(OH)3', 6H5', 6H3'), 3,64-3,53 (m, 14H, 1H2, 6H2', 1H5, 6H4'), 3,42-3,39 (m, 1H, NH), 3,09-3,03 (m, 1H, H4), 2,79-2,75 (m, 4H, H6, H7), 2,63-2,61 (m, 2H, H9), 1,71-1,68 (m, 2H, H8), 1,17 (t,  $J = 7$ Hz, 2H, NH<sub>2</sub>).

$^{13}C$ -NMR (125 MHz,  $D_2O$ , ppm):  $\delta$  101,9 (7C, 6C-1', 1C-1), 81,2 (7C, 6C-4', 1C-4), 72,1 (14C, 6C-2', 6C-3', 1C-2, 1C-3), 60,4 (6C, C-6'), 54,0 (C-6), 45,3 (C-7), 36,6 (C-9), 30,3 (C-8).

### 3.1.3 Synthesis of mono-6-(1,6-hexamethylenediamine)-6-deoxy- $\beta$ -cyclodextrin

Efficiency: 71%.

Appearance: The product is a white, fibrous solid crystal.

Melting point: 261-262°C

$R_f$  (butanol:ethanol:aq = 5:4:3) = 0,49.

QTOF-MS( $m/z$ ):  $[M+H]^+ = 1233,4870$  tương ứng với  $M = 1232,49$  (CTPT:  $C_{48}H_{84}N_2O_{34}$ )

IR ( $\nu_{max}$ ,  $cm^{-1}$ , KBr): 3331 (N-H), 2927(C-H), 1155 (C-O-C), 1239 (C-N), 1033 (C-O), 857 (C-C).

$^1\text{H-NMR}$  (500 MHz,  $D_2O$ , ppm):  $\delta$  5,46 (*s*, 7H, H1), 4,26-3,97 (*m*, 28H, 1(OH)2, 6(OH)2', 1(OH)3, 6(OH)3', 1H2, 6H2', 1H3, 6H3'), 3,78-3,77 (*m*, 7H, 1H5, 6H5'), 3,43 (*d*,  $J = 13,5\text{Hz}$ , 7H, 1H4, 6H4'), 3,13 (*m*, 2H, H6), 2,97 (*br, s*, 4H, H7, H12), 1,9-1,72 (*br, s*, 8H, H8, H9, H10, H11).

$^{13}\text{C-NMR}$  (125 MHz,  $D_2O$ , ppm):  $\delta$  102,4 (7C, 6C-1', 1C-1); 81,7 (7C, 6C-4', 1C-4); 72,1 (14C, 6C-2', 6C-3', 1C-2, 1C-3); 60,8 (6C, C-6'); 48,5 (C-6); 47,3 (C-7); 41,1 (C-12); 31,2 (C-11); 26,6 (3C, C-8, C-9, C-10).

### 3.2 3.2 Synthesis of drug-loaded nanocomposites

The results of the 5-FU drug compatibility test for nanosystems were carried out through the investigation of the drug content increasing gradually from 5% to 50% compared to the weight of the material. The results show that the complexation efficiency (%EE) of the drug and the drug tolerance of the material (%DL) are significantly influenced by the initial 5-FU ratio.

As for the drug tolerability of the materials, the results show that the materials have quite high drug loading rates, and there is a similarity in the rule of influence of  $\beta$ -CD derivatives on the % value. DLmax in two groups of materials. Specifically, the drug loading capacity of TAMCD derivatives reached the highest level at 68% in hybrid materials and 40.08% in nanogel materials, the lowest in HPCD derivatives with %DL values respectively. 23.46% and 32.12%. This shows that the presence of primary and secondary amine groups on the  $\beta$ -CD molecule has contributed to increasing the binding efficiency between drug molecules and materials, whereas the ether group can hinder the interaction between drug molecules and materials. they. Experiments also show that the centrifugation process is more favorable in TAMCD and  $\beta$ -CD derivatives, while HPCD with higher solubility should be more present in the solution which may have led to the loss of the product. exit 5-FU.

In another aspect, observing drug tolerance results in two groups of

materials (nanogel and nano hybrid) can see that the difference is not too large while the ratio of  $\beta$ -CD-x in the groups is significantly different. ( $\beta$ -CD-x accounts for a low percentage in nanogel materials and a superior proportion in hybrid materials). This result once again reinforces the initial assumption about the distribution of drug molecules in the polymer network or the whole organic layer on the surface of gold nanoparticles.

### **3.3 Physicochemical properties of nanocomposites**

#### **3.3.1 Nanogel systems based on $\beta$ -CD-x/alginate**

The presence of components in nanocomposites was determined through FT-IR spectroscopy of samples of  $\beta$ -CD-x, Alg, hollow materials and drug-loaded nanocomposite samples.

The results of FT-IR spectrum analysis of the 5-FU@ $\beta$ -CD/Alg nanocomposite sample showed that the signals have shifted to new positions compared to the  $\beta$ -CD/Alg carrier system. The wide signal at  $3413\text{ cm}^{-1}$  characterizes the dilatation of the O-H and N-H groups. The signal  $2934\text{ cm}^{-1}$  is typical for the stretching oscillation of the C-H group. The oscillations at  $1613\text{ cm}^{-1}$  and  $1424\text{ cm}^{-1}$  represent the C=O and -OH groups of alginate, respectively, and the signal at  $1034\text{ cm}^{-1}$  corresponds to the oscillations of the -C-O-C group in the glucose ring. In particular, the spectrum of the drug-loaded composites showed bands at  $1350 - 1250\text{ cm}^{-1}$  corresponding to the characteristic fluctuations of the C-N and C-F groups in the 5-FU molecule. The results confirmed that 5-FU was successfully bound to the  $\beta$ -CD-x/Alg . carrier.

The zeta potential and particle size are important criteria for assessing the potential for anticancer drug delivery and targeting efficacy in tumor tissue. The zeta potential and particle size analysis results of  $\beta$ -CD-x/Alg hollow materials and 5-FU@ $\beta$ -CD-x/Alg nanocomplexes are described in Table 3.4. Due to the negative zeta potential of the components  $\beta$ -CD-x and Alg [76], the hollow nanocomposite

$\beta$ -CD-x/Alg possesses a large surface charge (-48.7 mV to -70.2 mV), while the presence of 5-FU caused a slight decrease in surface charge (-42.1 mV to -62.2 mV). The high negative zeta potential induces repulsive interactions between the nanoparticles that can drastically reduce the nature of the tendency to coalesce, consistent with the high stability of the nanocomposites in aqueous solution. It indicates that  $\beta$ -CD-x and Alg-based nanocomposites can protect the drug as an ideal carrier for drug delivery system.

The particle size of nanocomposites in aqueous solution was determined through DLS measurement, the results showed that there were differences between materials. Specifically, the particle size of  $\beta$ -CD/Alg in the range of 50 - 150 nm with the average size of 70 nm, the HPCD/Alg materials possess the size in the lower range (40 - 200 nm) with the average size. 80 nm, while the TMACD/Alg particles are distributed in the larger size region (80 – 250 nm) with an average value of 120 nm. This shows that the substituents on the CD molecule have affected the complexation process with alginate chains and the critical equilibrium value on the nanoparticles surface. On the other hand, the results also showed a slight decrease in particle size in the loaded nanocomposites, the particle sizes of 5-FU@ $\beta$ -CD/Alg and 5-FU@TMACD/Alg were found in the range of 20 - 140 nm with an average size of 57 nm while the particle size of HPCD/Alg possesses a narrower range of 40 - 120 nm with an average size of 70 nm. The smaller size of the 5-FU@ $\beta$ -CD-x/Alg nanocomposite indicated that the presence of the drug 5-FU could significantly reduce the nanoparticle size, which confirmed the encapsulation of 5-FU to a cross-linking matrix forming calcium ions and alginate chains in  $\beta$ -CD-x/Alg nanocomposites.

The TEM image of the drug-containing nanocomposite samples shows that most of the drug-loaded nanoparticles are spherical with fairly uniform sizes distributed in the range of 40 - 120 nm, with high density in the 60 - 80 nm region.

In particular, it can be observed that the agglomeration between nanoparticles occurs more frequently in the 5-FU@HPCD/Alg and 5-FU@TMACD/Alg nanocomposites. This shows that the ether and amine groups on the  $\beta$ -CD molecule affect not only the complexation efficiency but also the stability of the nanogel in aqueous solution.

### 3.3.2 Hybrid gold nanomaterials

The structural characteristics of hollow nanomaterials and drug carriers were analyzed through FT-IR spectroscopy, the presence of drugs in the nanocomposites was demonstrated through characteristic absorption peaks on infrared spectrum and UV measurement results. -Vis.

Experimental results show that the pink-white hollow nanomaterial is obtained with the maximum absorption band at about 525 nm in the UV-Vis spectrum. Whereas nanocomposites containing 5-FU are blue solids that absorb at a wider wavelength (about 550 nm). The shift of the absorption peaks of the doping material shows a significant change of the AuNPs surface in the presence of 5-FU. It may be involved in the formation of a new stable organic film produced by the competition between the 5-FU/CD-x complex and the CD-x molecules for interaction with the gold nanoparticle surface. In particular, the UV-Vis spectrum of the drug-loaded nanocomposite clearly shows the absorption peak of 5-FU at about 266 nm, confirming the drug successfully loaded into the nanocomposite.

The FT-IR spectra of the hollow nanomaterials show that the characteristic absorption peaks of glucose molecules in cyclodextrin appear at peaks around 3420, 2940, 1640, 1414 and 1031  $\text{cm}^{-1}$ . The peaks at 3420  $\text{cm}^{-1}$  and 1414  $\text{cm}^{-1}$  are assigned to the stretching and bending vibrations of the OH groups, respectively. The peak at 2940  $\text{cm}^{-1}$  corresponds to the stretching vibration of alkyl C-H in the glucose molecules. The peak at 1640  $\text{cm}^{-1}$  is related to the stretching vibration of the C = O group and the peak at 1030  $\text{cm}^{-1}$  corresponds to the stretching vibration of the C-O



group. This result confirmed that all CD derivatives effectively hybridized with AuNPs particles. The spectrum of 5-FU drug shows peaks at 3151  $\text{cm}^{-1}$  and 2934-2832  $\text{cm}^{-1}$  due to N-H and C-H stretching oscillations, respectively. The peaks at 1769 - 1662  $\text{cm}^{-1}$  are related to the stretching oscillations of the C = O group and the peaks at 1350 and 1248  $\text{cm}^{-1}$  are characteristic of the oscillations of the C-N and C-F groups, respectively [77]. The FTIR spectra of the drug-loaded nanocomposites showed all characteristic peaks of both hollow nanomaterials (1414 and 1034  $\text{cm}^{-1}$ ) and 5-FU (1722, 1350 and 1248  $\text{cm}^{-1}$ ), this result confirms the presence of drugs in nanocomposites.

The crystal structures of 5-FU, hollow materials and drug-loaded nanocomposites were evaluated by XRD spectroscopy of the powdered samples. The XRD patterns of the hollow materials show characteristic peaks of AuNPs crystals at  $2\theta$  angles of 38.4°, 44.8°, 64.4° and 77.5°, ascribed to the face center mass (fcc) of (1 1 1), (2 0 0), (2 2 0) and (3 1 1). The XRD pattern of the drug 5-FU shows a crystalline structure with a strong intensity peak at an angle of  $2\theta$ , corresponding to 28.4°. The XRD data of the loaded nanocomposites show characteristic peaks for both 5-FU and AuNPs/CD-x nanocomposites. Furthermore, the peak intensity at  $2\theta$  28.4° is in the order of 5-FU@ AuNPs/TMACD > 5-FU@AuNPs/CD > 5-FU@AuNPs/HPCD, related to the content of 5-FU drug in sample, in accordance with the drug loading efficiency value of the material as mentioned in section 3.2.

SEM and TEM images of the loaded materials and nanocomposites were investigated to evaluate the effects of drug loading as well as different cyclodextrin derivatives on their morphology and particle size (Figure 3.12). SEM images indicated that there was no significant change in morphology between the cyclodextrin derivatives, however, a difference was clearly observed between the hollow material and the drug-loaded nanocomposite. Indeed, the hollow material

has a very smooth surface (Figures 3.12 A1, C1 and E1) while the surface of the drug-loading composites is rough (Figures 3.12 B1, D1 and F1). It is possible that the presence of 5-FU in the sample caused the more porous structure of the nanocomposite.

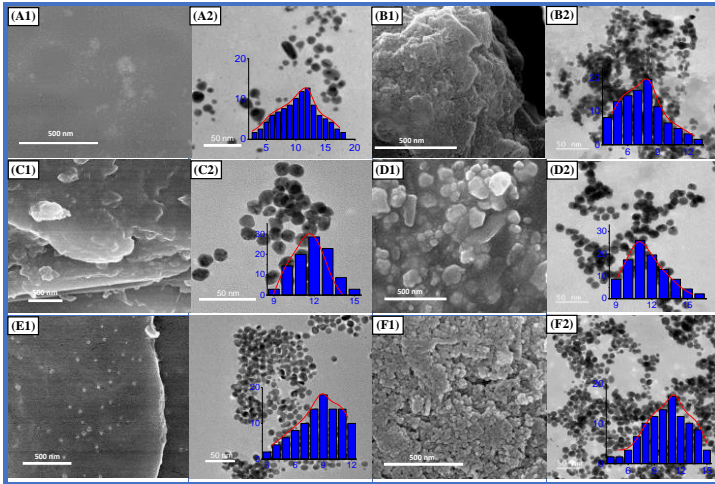


**Figure 3.12** SEM, TEM images and size distribution of nanocomposites: *AuNPs/CD (A1 and A2), 5-FU@AuNPs/CD (B1 and B2), AuNPs/HPCD (C1 and C2), 5-FU@AuNPs/HPCD (D1 and D2), 5-FU@AuNPs/DAPCD (E1 and E2) and 5-FU@AuNPs/TMACD (F1 and F2).*

TEM images show that the gold nanoparticles in all samples are spherical with slightly different size distributions. AuNPs/CD and AuNPs/TMACD samples exhibit a wide size distribution in the range of 3 - 18 nm while the size distribution of AuNPs/HPCD is within a narrow range of 9 -15 nm with the highest frequency distribution. is 12 nm. In addition, drug-loaded nanocomposites were also observed following a similar trend with different size distributions. 5-FU@AuNPs/CD and 5-

FU@AuNPs/TMACD show a wide band of 4 -13 nm with the highest frequency distribution of 8 nm and 4 - 15 nm with the highest frequency distribution respectively. 11 nm. The size of 5-FU@AuNPs/HPCD is distributed in the range of 9 - 16 nm with the highest frequency distribution of 11 nm. Notably, the TEM images of the hollow materials showed a decoupled distribution between the nanoparticles while the drug-loaded nanocomposites showed a significant aggregation between the nanoparticles. It is clear that the drug 5-FU caused a significant change in the surface plasmonic resonance (SPR) of AuNPs, which is consistent with the color change data in the UV-Vis spectrum.

### **3.4 Research results on drug release *in vitro***

#### **3.4.1 Release of 5-FU from nanogel materials**

Drug release studies from polysaccharide-based nanogel materials are often tested with physiological environments simulating blood, gastric or lower acidic environments because of the strong influence of environmental pH on structure and specificity. Calculation of complexes involving polysaccharide chains. In this study, the *in vitro* release processes of 5-FU from nanogel materials were performed in phosphate buffer pH 7.4 and 1.2.

The data show a high similarity between the materials in terms of drug release rates as well as kinetics. The analysis results by UV-Vis showed that the 5-FU content released from the nanosystems increased gradually over time and quite quickly in the first 12 hours and then gradually decreased. The drug release from the nanoparticles appears to have occurred in two stages: "sudden release" and "continuous release". The initial explosive phase may be due to drug absorption on the surface of the nanoparticle, while the slow release of the drug is due to matrix degradation and drug diffusion from the polymer matrix. Sudden release of the drug in the body ensures rapid reaching of therapeutically effective concentrations and prolonged release can cause the drug in the body to remain within the therapeutic

range of concentrations thereafter. The difference in drug release rates between the materials and the reference samples showed the advantage of long-term drug control of each material.

Comparing drug release rates in different media, the results show a clear difference in drug content as well as kinetic patterns at respective pH values. For medium (pH 7.4), drug release rates were 37.7% and 52.1% after 1 hour and 4 hours, respectively, reaching 69.8% after 24 hours and 80.7% after 96 hours. . Meanwhile, a much slower release rate was observed at pH 1.2 and the release rate reached only 20.0% in the first 4 hours and 34.1% in the next 96 hours. Therefore, the results indicate that 5-FU drug in CD-x/Alg nanocomposite is well protected in physiological environment, the drug release rate from nanocomposite can be adjusted by changing the environmental pH towards the target. Effectively applied to target cancer cells.

### **3.4.2 Release of 5-FU from AuNPs/CD-x nanocomposites**

In vitro drug release study of 5-FU was performed in PBS buffer at pH 7.4 and 1.2. The drug-loaded nanocomposites showed stable release in a non-linear pattern in which the percentages of drug release of 5-FU@AuNPs/CD, 5-FU@AuNPs/HPCD and 5-FU @AuNPs/TMACD after 24 h were determined to be  $31.26 \pm 0.62\%$ ,  $19.54 \pm 0.95\%$  and  $22.11 \pm 1.05\%$ , respectively. While at pH 1.2, the drug content released from the respective combinations was higher (respectively:  $36.54 \pm 0.24\%$ ,  $34.0 \pm 0.65\%$  and  $43.45 \pm$  respectively.  $0.85\%$ ). The small differences between cyclodextrin derivatives indicate the influence of functional groups on drug protection in nanocomposites. In contrast, for free 5-FU exhibits a relatively rapid release, reaching  $92.01 \pm 4.51\%$  after only 5 h. Compared with the drug release results based on cyclodextrin complexes previously reported [83,84], it is noteworthy that the nanocomposites in this study are more stable in the test environment. The high stability is due to the interaction between the drug and

the plasmonic surface of AuNPs which can interfere with the diffusion of the drug into solution. Thus, the drug is double protected during its delivery from the material in the physiological environment.

### 3.5. Cytotoxicity assay

For the nanogel group, the results of cytotoxicity assessment on two cell lines (normal cell fibroblasts and breast cancer cell line MCF-7) showed that the  $\beta$ -CD-x-based nanosystems were uniform. was not inhibitory to either cell lines. While the drug solution released from the nanosystems was relatively potent on the MCF-7 cell line with an inhibition rate of 70 to 80%.

Cytotoxic effects of  $\beta$ -CD/Alg nanomaterials; 5-FU@ $\beta$ -CD/Alg and solutions released at different pH values after 48 h. As can be seen, the hollow nanocomposites had no inhibition on the normal cell line but a slight inhibition of  $26.83 \pm 3.58$  against the cancer cell line at the concentration of 100  $\mu\text{g/mL}$ . However, the IC<sub>50</sub> value of  $\beta$ -CD/Alg was more than 100  $\mu\text{g/mL}$  for both cell lines, demonstrating the high biocompatibility of the carrier material. Furthermore, the inhibition of 5-FU against cells are usually about  $45.31 \pm 5.52\%$  (concentration 100  $\mu\text{g/mL}$ ) much higher than the 5-FU@ $\beta$ -CD/Alg nanosystem. This result demonstrates the limitations of using the standalone 5-FU drug in chemotherapy without a drug delivery system. On the other hand, the 5-FU@ $\beta$ -CD/Alg nanocomposite showed high toxicity to cancer cell lines but almost no toxicity to normal cells. Indeed, the 5-FU@ $\beta$ -CD/Alg nanosystem inhibited  $71.75 \pm 3.73\%$  for MCF-7 cells and  $20.59 \pm 3.07\%$  for fibroblasts, respectively, while IC<sub>50</sub> values are  $21.68 \pm 2.22 \mu\text{g/mL}$  and  $\geq 100 \mu\text{g/mL}$  respectively. These results indicate that nanocomposites are safe for normal cells but have very good resistance against cancer cells.

To evaluate the drug release effect from the nanocomposite, the toxicity of the solution after release at pH = 7.4 and pH = 1.2 after 48 h was tested for both cell

lines. Good toxicity of these release solutions was detected for MCF-7, with inhibition of  $78.48 \pm 0.97\%$  at pH = 7.4 and  $70.32 \pm 0.98\%$ , respectively.  $IC_{50}$  values of  $2.02 \pm 0.38 \mu\text{g/mL}$  and  $10.96 \pm 0.69 \mu\text{g/mL}$  respectively, while this solution shows very low toxicity to normal cells. In addition, statistical analysis of the data showed that the  $IC_{50}$  value of 5-FU nanocomplex @ $\beta$ -CD/Alg released at pH = 7.4 inhibited MCF-7 similar to 5-FU alone. but significantly different from the solution liberated at pH = 1.2. The results therefore suggest the safety and high potential of using  $\beta$ -CD and  $\beta$ -CD-based nanomaterials modified with alginate as an anticancer drug delivery system with activity Highly antiproliferative to intravenous MCF-7 cells and safe to normal healthy cells.

In the hybrid gold nanogroup, the cytotoxic activity of hollow nanomaterials and drug-loaded nanocomposites was investigated. It can be seen that all hollow nanomaterials do not inhibit normal cells and cancer cells, which demonstrates the high biocompatibility of materials based on AuNPs and cyclodextrin.

Meanwhile, the drug-loaded nanocompounds showed different bioactivity against cell lines and depended on the structure of cyclodextrin derivatives. The 5-FU@AuNPs/HPCD sample exhibited low antitumor bioactivity ( $33.42 \pm 4.73\%$ ) and did not inhibit normal cells while 5-FU@ AuNPs/TMACD showed high activity against normal cells. with both cell lines ( $90.27 \pm 1.64\%$  for MCF-7 and  $40.92 \pm 2.89\%$  for fibroblasts). Nanocomposite, 5-FU@AuNPs/CD showed the ability to inhibit cancer cells ( $54.00 \pm 5.21\%$ ) but not normal cells. Although the biological activity of 5-FU@AuNPs/CD against MCF-7 cells ( $IC_{50}$  value =  $16.04 \pm 1.76 \mu\text{g/mL}$ ) was slightly lower than that of 5-FU@AuNPs/TMACD ( $IC_{50}$  value =  $23.66 \pm 4.76 \mu\text{g/mL}$ ), but it is safer for normal healthy cells. The difference in the antitumor activity of the nanocomposites is due to the different loading efficiency values of 5-FU in the samples. This result shows an advantage over 5-FU when

loaded onto AuNPs/CD materials and suggests that among them AuNPs/ $\beta$ -CD and AuNPs/TMACD nanocomposites should be preferred as a Potential 5-FU drug delivery system for breast cancer treatment.

## IN CONCLUSION

From the presented research results, we draw the main conclusions of the thesis including:

1. The amine derivatives of  $\beta$ -CD including CD-NH<sub>2</sub>, TMACD, HMACD have been synthesized by microwave irradiation technique with the respective yield of 63.96%; 76.5% and 68%.

2. Successfully synthesized nanoparticles based on modified  $\beta$ -CD and  $\beta$ -CD with two specific structures: Nanogel ( $\beta$ -CD-x/alginate) and hybrid nanoparticle (AuNPs/ $\beta$ -CD-x). The factors affecting the material synthesis process have been optimized with efficiency ranging from 86.5% to 92.5%.

3. Tests to carry cancer drug 5-Fluorouracil onto materials have been carried out. The complexation efficiency and drug tolerability of 5-Fluorouracil on the materials were relatively high, in which the TMACD-based materials showed the best drug loading ability, followed by the  $\beta$ -based materials. -CD and lowest in HPCD materials. The DL<sub>max</sub> value ranges from 23.5% to 68%.

4. The structure of nanoparticles and drug-carrying nanocomplexes was demonstrated by spectroscopic methods. Morphology, particle size, crystal structure, physicochemical characteristics of nanomaterials and drug-carrying nanocomplexes as well as the stability of nanosystems analyzed by modern techniques, size of materials nanogel in the range of 40 to 250 nm and 15-120 nm in hybrid materials, the zeta potential in aqueous solution from -42mV to -70mV.

5. Kinetics of drug release processes from nanosystems under different conditions were investigated. The law of drug release in simulated physiological

environments has been studied. Under pH 7.4 conditions, drug release from nanogel materials reached 68% after the first 24 h and reached a maximum of 80% at the next 96 h. In hybrid nanomaterials, the amount of 5-FU released after 24 hours reached 19.6% to 31%.

6. Cytotoxicity of nanomaterials, drug-carrying nanocomplexes and drug-release solutions were tested on normal cell lines (fibroblasts) and breast cancer cell lines (MCF-7). The results show the safety and high potential of using modified  $\beta$ -CD and  $\beta$ -CD-based nanomaterials as an anticancer drug delivery system with high antiproliferative activity against MCF-7 cells and had negligible effect on normal healthy cells.

### **RECOMMENDATIONS**

Research on developing a range of drug delivery nanomaterials based on modified  $\beta$ -CD and  $\beta$ -CD initially shows many advantages and limitations that need to be improved. Therefore, it is necessary to expand the research chain on other derivatives of  $\beta$ -CD (amide; thiol...) and to test the combination on other polymer platforms such as CMC; Chitosan, PEG...will provide a more complete data set for this research direction.

Drug delivery efficiency can be tested on a group of drugs or anti-cancer precursors of medium or larger size: Letrozole; Paclitaxel... Preparation of drug-delivery materials with targeted functions is of recent scientific interest. The next step of the hybridization process needs to be researched to attach the target center to the material in order to optimize the treatment effect and reduce the side effects on normal cells.

Research on drug release over a wide range of pH values simulating physiological environment will provide more complete kinetic data of drug release processes, towards the ability to actively adjust environmental pH to interfere with cells. targeted cancer cells.



## CONTRIBUTION OF THIS STUDY

The amine derivatives of  $\beta$ -CD including CD-NH<sub>2</sub>, TMACD, HMACD synthesized by microwave irradiation technique have allowed to shorten the reaction time and improve the efficiency compared with thermal processes.

For the first time, a group of nanomaterials based on modified  $\beta$ -CD and  $\beta$ -CD have been synthesized and successfully applied for the purpose of 5-FU cancer drug delivery. The results from the project will add more knowledge to the field of drug delivery nanomaterials.

Research results on the conditions for creating hybrid gold nanosystems with  $\beta$ -CD derivatives and their specific properties will contribute to the development of hybrid metal nanomaterials applied in the field of medicine.

Kinetics of 5-FU release processes from nanosystems provide data for further studies on CD-based drug delivery nanomaterials and CD derivatives.

The results of the cytotoxicity study show the safety and high potential of using modified  $\beta$ -CD and  $\beta$ -CD-based nanomaterials as an anticancer drug delivery system with high antiproliferative activity against MCF-7 cells and negligible effect on normal healthy cells.

## PUBLICATIONS RELATED TO THIS STUDY

### NATIONAL JOURNAL

Nguyễn Cao Hiền, Đinh Phước Lộc, Nguyễn Công Hào, Đặng Chí Hiền, Nguyễn Thành Danh\*, Synthesis of hydroxypropyl- $\beta$ -cyclodextrin/alginate nanosystem as a carrier for the cancer drug anastrozole. *Vietnam journal of chemistry* 5e34 (55) 2017.

Nguyễn Cao Hiền, Trần Minh Trọng, Lục Văn Siêu, Nguyễn Thành Danh, Đặng Chí Hiền\*, Synthesis of mono-6-amino-deoxy-6- $\beta$ -cyclodextrin derivatives applied in the preparation of gold nano. *Vietnam journal of chemistry* 6E1,2 (57) 2019.

### INTERNATIONAL JOURNAL

Thanh-Danh Nguyen\*, Thanh-TrucVo, Cao-Hien Nguyen, Van-Dat Doan, Chi-Hien Dang, Biogenic palladium nanoclusters supported on hybrid nanocomposite 2-hydroxypropyl- $\beta$ -cyclodextrin/alginate as a recyclable catalyst in aqueous medium. *Journal of Molecular Liquids* (2019) **276**, 927–935 [Q1]

Thanh-Danh Nguyen\*, Thanh-Truc Vo, T. Thanh-Tam Huynh, Cao-Hien Nguyen, Van-Dat Doan, Dinh-Truong Nguyen, Trinh-Duy Nguyen and Chi-Hien Dang, Effect of capping methods on the morphology of silver nanoparticles: study on the media-induced release of silver from the nanocomposite  $\beta$ -cyclodextrin/alginate, *New J. Chem.*, (2019) **43**, 16841-16852 [Q1]

Cao-Hien Nguyen, Kien-Sam Banh, Chi-Hien Dang\*, Cong-Hao Nguyen, Thanh-Danh Nguyen\*,  $\beta$ -cyclodextrin/alginate nanoparticles encapsulated 5-fluorouracil as an effective and safe anticancer drug delivery system. *Arabian Journal of Chemistry* (2022) **15**, 103814 [Q1].

Cao-Hien Nguyen, Kien-Sam Banh, Van-Dung Le, Minh-Ty Nguyen, Chi-Hien Dang\*, Tran Vinh Thien\*, Van-Dat Doan, DongQuy Hoang, Tran Thi Kim Chi, Thanh-Danh Nguyen\*, Ultrasound-assisted synthesis of gold nanoparticles supported on  $\beta$ -cyclodextrin for catalytic reduction of nitrophenols. *Inorganic Chemistry Communications* 145 (2022) 109979 [Q2].